A Human Physiologically-Based Model for Glycyrrhzic Acid, A Compound Subject to Presystemic Metabolism and Enterohepatic Cycling

Bart Ploeger,[1,5,6] Tjeert Mensinga,[2,3] Adriënne Sips,[4] Jan Meulenbelt,[2,3] and Joost DeJongh[5]

Received June 21, 2000; accepted September 9, 2000

Purpose. To analyze the role of the kinetics of glycyrrhizic acid (GD) in its toxicity. A physiologically-based pharmacokinetic (PBPK) model that has been developed for humans.

Methods. The kinetics of GD, which is absorbed as glycyrrhetic acid (GA), were described by a human PBPK model, which is based on a rat model. After rat to human extrapolation, the model was validated on plasma concentration data after ingestion of GA and GD solutions or licorice confectionery, and an additional data derived from the literature. Observed interindividual variability in kinetics was quantified by deriving an optimal set of parameters for each individual.

Results. The *a-priori* defined model successfully forecasted GA kinetics in humans, which is characterized by a second absorption peak in the terminal elimination phase. This peak is subscribed to enterohepatic cycling of GA metabolites. The optimized model explained most of the interindividual variance, observed in the clinical study, and adequately described data from the literature.

Conclusions. Preclinical information on GD kinetics could be incorporated in the human PBPK model. Model simulations demonstrate that especially in subjects with prolonged gastrointestinal residence times, GA may accumulate after repeated licorice consumption, thus increasing the health risk of this specific subgroup of individuals.

KEY WORDS: glycyrrhizic acid; modeling; enterohepatic cycling; PBPK; pharmacokinetics.

INTRODUCTION

Glycyrrhizic acid (GD) is of interest for the treatment of chronic hepatitis, since long-term administration of this compound reduces the development of hepatocellular carcinomas in this disease (1). Due to its sweet taste, approximately 50 times sweeter than sucrose, GD is also applied as a sweetener in a diversity of food products and in chewing tobacco (2). When considerable doses of GD are consumed habitually, mineral corticoid excess-like side effects may occur due to the inhibition of the enzyme 11-β-hydroxysteroid dehydrogenase (11-β-HSD) by its main metabolite, glycyrrhetic acid (GA) (3). In case of overconsumption, this may lead to hypertension, edema, and electrolyte disturbances. The differences in susceptibility for licorice-induced adverse effects between subjects might be due either to interindividual differences in the pharmacokinetics or in the pharmacodynamics of GD, or a combination of both (2). For the identification of the subgroups that are at higher risk for licorice-induced adverse effects, a detailed insight into these relationships is essential.

Over the past 15 years, physiologically-based pharmacokinetic (PBPK) models have been applied for the risk assessment of several xenobiotics (4,5). Due to a realistic anatomical and physiological representation of the organism, data from *in vitro, in vivo,* and *in situ* studies can be used to describe the kinetics of a compound *in vivo.* In addition, PBPK models can be readily scaled from one species to another. Moreover, the biological fate of a chemical can be predicted under a variety of exposure situations. Hence, PBPK models are useful for risk assessment purposes, since the actual exposure is often different from the exposure in the experimental setting. In combination with a quantitative relationship between the biologically active dose and its toxic effect(s), an adequately validated model may elucidate why and under which circumstances some subgroups of the population are more at risk than others (4,6).

The aim of the present study is to develop and validate a human PBPK model for GD, based on a previously developed rat model (7). In study in healthy volunteers on the pharmacokinetics of GD after consumption of a suspension of GA, a solution of GD or two different types of licorice confectionery was performed to calibrate this model. Moreover, information on the interindividual distribution of the model parameters that have the most influence on the model forecast was obtained from this study. The model was validated by comparison of its forecast with the results of previously published clinical studies. Finally, the impact of the model parameters on the pharmacokinetics of GD is discussed and is used to identify subgroups of subjects at risk for GD-induced adverse effects.

METHODS

Model Description

It is assumed that the structural PBPK model, which has been developed previously to describe the pharmacokinetics of GD and its main metabolite glycyrrhetic acid (GA) in rats (7), can also be applied to describe the kinetics of both compounds in humans (Fig. 1). GD is absorbed as its aglycon GA after enzymatic hydrolysis by commensal bacteria (Eqs. 21–23; see Appendix). In addition to the observation that GA is 200–1000 times more potent an inhibitor of 11-β-HSD *in vitro,* the kinetics of GA are of interest after oral GD treatment. GA distribution into body tissues other than the liver is minimal (Eq. 1–6). Following hepatic uptake by capacity limited carriers, GA is metabolized to mainly glucuronide metabolites. The observed rapid excretion of GA metabolites

[1] LAP&P Consultants BV, Kenniscentrum Archimedesweg 31, 2333 CM, The Netherlands.
[2] National Poisons Control Centre, National Institute of Public Health and the Environment, P.O. Box 1, 3720 BA, Bilthoven, The Netherlands.
[3] Department of Intensive Care and Clinical Toxicology, University Medical Centre Utrecht (UMCU), Utrecht, The Netherlands.
[4] Laboratory for Exposure Assessment and Environmental Epidemiology, National Institute of Public Health and the Environment, P.O. Box 1, 3720 BA, Bilthoven, The Netherlands.
[5] Leiden Advanced Pharmacokinetics & Pharmacodynamics (LAP&P) Consultants, Leiden, The Netherlands.
[6] To whom correspondence should be addressed. (e-mail: b.ploeger@lapp.nl)

0724-8741/00/1200-1516$18.00/0

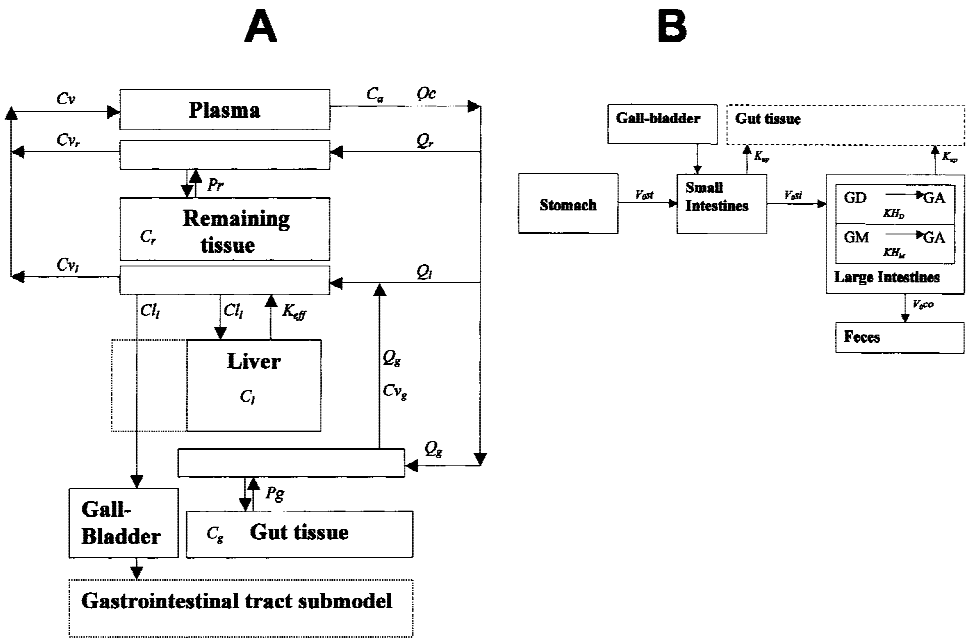

Fig. 1. Physiologically-based pharmacokinetic model for the systemic kinetics of GA in humans (panel A). Panel B represents the human gastrointestinal tract submodel (stomach and small and large intestines).

(GM) can only be explained if is assumed that GA is metabolized instantaneously, and that its metabolites are subsequently excreted into the bile (7). This suggests involvement of binding proteins, like 3-α-hydroxysteroid dehydrogenase, which prevent the reflux of the conjugates to plasma. The biliary excretion of GM is facilitated by the canalicular multispecific organic anion transporter (cMOAT). In the rat model, the hepatobiliary clearance of GA was described adequately on the assumption that the rate of hepatic uptake of GA and biliary excretion of GA metabolites are equal (Eq. 16, 17). Biliary excreted GA metabolites (GM) are, once excreted into the duodenum, reconverted into GA by bacteria in the gastrointestinal tract (Eq. 24) and subsequently reabsorbed into the systemic circulation (Eq. 6).

To overcome the lack of reliable data on human gastrointestinal lumen volumes, the four physiological compartments (stomach, small intestine, cecum, and colon) of the gastrointestinal tract model for rats were lumped into three compartments, representing the stomach and the small and large intestines (Fig. 1B). In humans, the gastric emptying and the transit time in the intestines has been measured by gamma scintigraphy and is generally defined as the time in which 50% of the contents pass the specific gastrointestinal compartment (8–11). It is assumed that the contents of the gastrointestinal tract pass with a constant (zero order) rate (Eq. 7–15). In the human model, biliary excreted GA metabolites are stored in the gall bladder and are excreted instantaneously into the gut after the ingestion of a meal containing fat (Eq. 18–20) (12).

Clinical Study

Human data on the pharmacokinetics of GA after oral administration of glycyrrhizic acid were obtained by performing a clinical study in conformity with the current rules for Good Clinical Practice (GCP). All subjects (8 males and 8 females) refrained from consuming food products containing GD within a 72 hour period foregoing product administration and during the entire study. In a 4-way random crossover design, subjects received four treatments (with a two week wash-out period): I) an aqueous suspension of 130 mg GA (equivalent to 225 mg GD) in 250 ml water-propyleneglycol (80-20% v/v); II) an aqueous solution (250 ml) of 225 mg GD; III) 150 g sweet (unsalted) licorice confectionery containing 225 mg GD; and IV) 150 g salted licorice confectionery, containing 225 mg GD and 5% w/w NH_4Cl. GA and the monoammonium salt of GD were purchased from Acros Chimica (Geel, Belgium), and Red Band Venco BV (Rozendaal, The Netherlands) kindly supplied the sweet and salted licorice. Food consumption was recorded during the first 24 hours. It took place at 4, 6, and 9 hours post-dosage. Blood was sampled at –1 (baseline), 2, 2.5, 4, 5.5, 7, 8.5, 10, 11.5, 13, 14.5, 18, 22, 32, 48, and 56 hr after the product administration. The blood samples were centrifuged immediately after sampling and the plasma was stored at –20°C until analysis. The GA plasma concentrations were determined by high performance liquid chromatography (HPLC) analysis. Briefly, GA was extracted from plasma by solid-phase extraction, using a C18 column. For the HPLC analysis of GA, a reversed phase C18 column and a gradient system of 78%–83% v/v methanol/water acidified with 0.3% acetic acid was used. GA was detected at 250 nm. All chemicals used in the HPLC analysis were of analytical grade and were purchased from Merck (Darmstadt, Germany).

Model Calibration

The values of the anatomical and physiological parameters were obtained from literature (Table I). In the literature, the gastric emptying time of nonsolid material ranged from 0.12 to 0.62 hr (mean 0.38 hr) (9,11), whereas the gastric emptying time of a solid formulation ranged from 0.13–3.51 hr (mean 1.83 hr) (8–11). There is no difference in the small intestinal transit time between liquid or solid formulations (9,10), and the transit time in the small and large intestines is

Table 1. Abbreviations of the Parameters of the Human Physiologically-Based Pharmacokinetic Model for Glycyrrhizic Acid (GD)

Abbreviation	Parameter
A_{gb}	Amount (mg) GM stored in gall bladder
A_l	Amount (mg) GA in the liver
As_x	Amount (mg) undissolved GA in small and large intestines (x = ti) and feces (x = fe)
$Adis_{ti}$	Amount (mg) GA which is dissolved in the small intestine
$A_{x,ti}$	Amount (mg) GM (x = M) or hydrolyzed GD or GM (x = DM) in the small and large intestines
$A_{x,fe}$	Amount (mg) GA (x = A) or GD (x = D) in feces
BW	Body weight (kg)
Cl_l	Plasma to liver and plasma to bile clearance ($L \cdot hr^{-1}$)
Cl_lC	Plasma to liver and plasma to bile clearance ($L \cdot hr^{-1} \cdot kg^{-1}$ liver weight)
Cs	Solubility GA in small intestine ($mg \cdot L^{-1}$)
C_x	Concentration ($mg \cdot L^{-1}$) GA in venous (x = v), arterial (x = a), venous liver (x = vl), liver (x = l), gut (x = g) or remaining tissue
$Dose_x$	Oral dose (mg) GA (x = A) or GD (x = D)
f_u	Fraction unbound
K_{eff}	Hepatic efflux (hr^{-1})
KH_x	First order hydrolysis rate constant (hr^{-1}) of GD (x = D) or GM (x = M)
Km	Apparent Michaelis–Menten constant ($\mu mol*L^{-1}$)
Ks	Dissolution clearance GA in small intestine ($L \cdot hr^{-1}$)
K_{up}	First order GA uptake rate constant (hr^{-1}) in the small and large intestines
$K_{up,x}C$	Allometrically scaled ($K_{up,x} = K_{up,x}C*BW^{-0.3}$) first order GA uptake rate constant (hr^{-1} – 1 kg animal) in small (x = si) and large (x = co) intestines
n_{cap}	Number of capsules
P_x	Partition coefficient for gut (x = g) or remaining (x = r) tissue
Q_c	Cardiac output ($L \cdot hr^{-1}$)
Q_x	Perfusion rate ($L \cdot hr^{-1}$) of liver by hepatic artery (x = l), portal vein (x = g), or remaining tissue (x = r)
T ½ x	time (hr) in which 50% of the contents is emptied from the stomach (x = st) or passed the small intestines (x = si), the large intestine (x = co), or the small and large intestines together (x = ti)
V_0 st	Zero order gastric emptying rate ($mg \cdot hr^{-1}$)
V_0 x	Zero order transit rate of gastrointestinal contents through small (x = si) and large intestines (x = co) ($mg \cdot hr^{-1}$)
V_{co}	Volume of contents in the small intestine (L)
$V_{max}C$	Maximum plasma to liver and plasma to bile transport rate ($\mu mol \cdot hr^{-1} \cdot kg^{-1}$ liver weight)

found to be 3 hr (8–11) and 14.9 hr (13), respectively. The hydrolysis rate of GD and the glucuronide metabolites of GA by commensal bacteria in humans were obtained from an *in vitro* study (14). The values for the remaining tissue-to-plasma (Pr) and gut tissue-to-plasma (Pg) partition coefficients and the first order hepatic efflux rate (K_{eff}) were taken from the rat model (Table II). Based on a study with rat and human vesicles of the canalicular membrane (15) it is expected that the maximum hepatic transfer rate of GA ($V_{max}C$) in humans is a factor 3 times lower than in rats. In addition, the apparent Michaelis–Menten constant K_m in humans is assumed to be 14.5 times lower than in rats, since the fraction GA unbound is lower in humans than in rats (16). However, the human calibration data set contains only plasma concentration-time data after a single dose treatment, and $V_{max}C$ and K_m cannot be identified simultaneously. Therefore, the ratio of both, being the constant clearance rate ClC, was adjusted to the data. For the two remaining parameters that describe the GA uptake clearance from the small ($K_{up,si}C$) and large ($K_{up,co}C$) intestines, no information on specific interspecies differences is available and were therefore allometrically scaled by $BW^{-0.3}$ (17) (Table III). To forecast the emptying of the gall bladder, the daily times at which a meal containing fat was consumed were estimated based on food-intake recordings during the first 24 hours of the experiment. It was assumed that the gall bladder emptied at 4, 6, 9, 21, 27, 33, 45, 51, and 57 hours after the treatment.

Sensitivity Analysis

Using a normalized sensitivity analysis (18) in which the percentage change in the area under the plasma concentration time-course (AUC) of GA was calculated as a result of one percentage change in a model parameter, it can be determined whether model parameters contribute substantially to the model forecast. Parameters that show a low sensitivity can be eliminated from the model without loss of predictability (18).

Interindividual Variance

The interindividual variability in the GA kinetics, observed in present study, can be quantified by deriving an optimal set of parameters for each individual, followed by a statistical analysis of their distributions. Four parameters of the GA model can be identified simultaneously, since only GA plasma concentration data is available (7). It can be assumed that most of the interindividual variance will be explained by the parameters that have the most influence on the model forecast. To reduce the correlation between the optimized parameters resulting in imprecise parameter estimates, the parameters were optimized simultaneously on the pooled data of the GA treatment, the GD solution, and the sweet and salted licorice confectionery, respectively. Hence, for the 16 subjects, 3 parameter sets were derived. A proportional error

Table 2. Physiological Parameters of the Physiologically-Based Pharmacokinetic Model Glycyrrhetic Acid (GA) in Humans

Parameter		Source
Volumes (fraction of body weight)		
Liver tissue	0.026	(28)
Gut tissue	0.017	(28)
Remaining tissue	0.825	(28)
Total blood volume	0.0815	(29)
Volumes (fraction of total blood volume)		
Venous blood	0.615	(28)
Arterial blood	0.19	(28)
Volume blood in tissue (fraction of tissue weight)		
Liver	0.15	(28)
Flows (l/hr)		
Cardiac output	312	(29)
Tissue blood flows (fraction of cardiac output)		
Liver (portal vein)	0.06	(28)
Liver (hepatic arteria)	0.19	(28)
Other Parameters		
Fraction unbound	0.0006	(16)
Volume of contents Small intestines (L)	0.4	(29)
Hematocrit	0.42	(29)

model was used to account for the error in the experimental GA plasma concentration data. To determine the goodness-of-fit of the model and to assure independent estimation of the parameters, the correlation between the fitted parameters was monitored. New parameter starting values were chosen to obtain an absolute minimum in the log likelihood (LLK) function, if necessary. Finally, the parameter fit was evaluated by analyzing the random distribution of the weighted residuals of the observed and forecasted GA plasma concentration by a sign test on the probability of randomly distributed residuals (19).

Validation

The human GA model was evaluated by comparison of its forecasted AUC and C_{max} of GA with the observed values from a validation data set (Table IV). Comparison of predicted and estimated AUC and C_{max} were selected, since these kinetic parameters were reported in all studies of the validation data set. To simulate the GA plasma kinetics of GA in its undissolved form, the optimized human model was extended with the Noyes–Whitney equation (20) that describes the dissolution of poorly soluble compounds (Eq. 25). Following gastric emptying of undissolved GA in the duodenum (Eq. 26), some of the GA particles will dissolve with a dissolution rate that is calculated from this equation (Eq. 27). The remaining undissolved GA particles will be cleared from the small intestinal tract with a half-life of 3 hrs (Table III) (Eq. 28). The dissolution clearance (K_S), which is assumed to be proportional to the number of capsules administered (Eq. 25), and the solubility of GA in the small intestine are both unknown and will be optimized to the pooled mean plasma concentration after the administration of 500, 1000, or 1500 mg GA (21).

Model Simulations

The percentage of the dose GA or GD after a GA suspension, a GD solution, or GD as sweet or salted licorice confectionery that is absorbed, is calculated from the fraction of the dose that appears unchanged in the feces (F_{fe}). The fraction absorbed (F_a) can be derived from:

$$F_a = (1 - F_{fe}) \quad \text{(Eq. 29)}$$

Statistical Analysis

The estimated individual parameter values per treatment were tested on normality or log-normality, using the Kolmogorov–Smirnov test (19). Parameter values that fell well away from the main parameter distribution were not used for further statistical analysis to warrant optimal parameter sets (19). On the condition of equal variances, parameter distributions were compared using the one-way analysis of variance followed by a Tukey honestly significant difference test. Statistical significance is considered present at $p < 0.05$. For the statistical tests, SPSS for Windows (release 7.5.2; SPSS Inc.) was used.

Simulation Software

The model equations (see Appendix) were coded in ACSL for Windows (version 11.4.1; MGA software Inc.). Electronic copies of the ACSL model code are available from the authors. For the optimization of the model to the individual data, the Nelder–Mead (simplex) algorithm of ACSL Math (version 1.2; MGA software Inc.) was used. The normalized sensitivity coefficients of the model parameters were calculated with the sensitivity module of ACSL Math after multiplying the output with the value of the model parameter.

RESULTS

After extrapolation of all relevant parameters from rat to human, it was possible to describe the mean experimental GA plasma concentration data after the GA suspension treatment adequately fit with the model (Fig. 2A). All parameters of this model were defined *a priori.* The predicted plasma concentrations in the terminal phase after oral administration of the GD solution and the two licorice confectionery treatments were slightly higher than observed (Fig. 2 B, C and D). The C_{max} levels after the two licorice treatments closely resembled the observed value, whereas the C_{max} after the GD solution was clearly overestimated by the *a priori* defined model.

During the first hours after the oral administration of a GA suspension $K_{up,si}C$ had the most influence on the AUC, whereas during the last 24 hours of the simulation the $K_{up,co}C$ showed the highest sensitivity coefficients (Fig. 3 A). T½si showed low sensitivity coefficients after a GA treatment (Fig. 3 B). The parameter $K_{up,si}$ had no influence on the AUC after the oral administration of GD (data not shown). Due to the limited influence of $K_{up,si}C$ and T½si on the forecast of the plasma concentration of GA after either an oral GA or GD dose, the compartments that represent the small and large

Table 3. Biochemical Parameters of the Physiologically-Based Pharmacokinetic Model for Glycyrrhetic Acid (GA) in Humans

Parameter	*A priori*	Source	Treatment			
			139 mg GA (suspension) (n = 15)	225 mg GD (solution) (n = 15)	150 g sweet licorice (n = 14)	150 g salted licorice (n = 15)
$Cl_1C^a(\cdot 10^4)$	1.10	Rat model	1.33 (1.09–1.61)	1.30 (0.87–1.92)	1.43 (0.99–2.06)	1.27 (1.09–1.61)
Cs	$1.21 \cdot 10^4$	Optimized				
K_{eff}	1.26	Rat model	1.26	1.26	1.26	1.26
$KH_D{}^a$	0.10	(14)	0.11 (0.09–0.15)	0.07 (0.05–0.11)	0.15 (0.09–0.25)	0.14 (0.10–0.21)
KH_M	0.05	(14)	0.05	0.05	0.05	0.05
Ks	0.23	Optimized				
$K_{UP}{}^a$	0.22	Rat model	0.22 (0.17–0.29)	0.18 (0.12–0.28)	0.29 (0.17–0.50)	0.21 (0.14–0.32)
Pg	0.06	Rat model	0.06	0.06	0.06	0.06
Pr	0.11	Rat model	0.11	0.11	0.11	0.11
T½st		See text	0.38	0.38	1.83	1.83
T½ti[a]	17.9	See text	17.7 (14.2–22.0)	21.0 (14.1–31.1)	17.1 (11.2–26)	15.4 (5.7–78)

[a] Optimized parameters, presented as mean with the 95% confidence interval in parentheses.

intestines could be lumped without loss of predictability. After lumping, the kinetics of GD and GA in the small and large intestines were described by four parameters, being K_{up}, KH_D, KH_M, and the time in which 50 percent of the contents passed the small and large intestines (T½ti). This T½ti was assumed to be 17.9 hr, being the sum of the T½si (3 hr) and the T½co (14.9) of the three compartmental model. Using a K_{up} of 0.22 (being the mean of the $K_{up,si}$ and $K_{up,co}$ of a person of 72 kg), the forecasts of the two and three compartment gastrointestinal model were comparable (data not shown). The parameters Cl_1C, T½ti, KH_D, and K_{up} showed the most influence on the forecast of the AUC of GA after either oral administration of GA or GD. These parameters were optimized to fit the individual data. The remaining parameters were kept fixed at their *a priori* values (Tables II and III).

The forecast improved after optimization of the four most sensitive model parameters in comparison with the *a priori*-defined model, especially for the simulation of C_{max} and T_{max} after the treatment of GD in solution. The observed and predicted GA plasma concentrations closely resembled each other and the weighted residuals were normally distributed around zero (Fig. 2).

After ^{10}log transformation, all parameter sets were normally distributed. The mean of the optimized individual parameters closely resembled their *a priori* values (Table III). A significant difference between the KH_D, of the GD solution and both licorice confectionery treatments was observed.

The GA kinetics after treatment of 200 mg GD as licorice confectionery (22) were simulated using the mean parameter values of the licorice treatment subsets. The two studies in which low doses of GD were administered (23,24) were simulated with the GD solution parameter subset. The model could adequately forecast the observed C_{max} and AUC (Table IV). Using the mean of the optimized parameter values (GA subset; Table III), the GA dissolution clearance (Ks) and solubility (Cs) in the small intestine was adequately fitted to the GA plasma concentration data after 500, 1000, and 1500 mg, respectively (21) (Fig. 4) (Table IV).

After the administration of 130 mg GA as suspension, the model predicted that 69% ± 20.6% (mean ± SD) of the dose was absorbed. This fraction was not significantly differ-

Table 4. The Relative Residuals Between Observed and Forecasted C_{max} and AUC After Various Oral Treatments with Either Glycyrrhizic Acid or Glycyrrhetic Acid

Compound	Matrix	Dose (mg)	n	Body weight (kg)	Food intake (post dosage time) (hr)	Relative residual (%)		Source
						AUC	C_{max}	
GD	Herbal preparation	23.2	6	NR[a]	4, 10, 24, 28, 34[b]	–10	–16	(23)
GD	Herbal preparation	27.4	5	60 (55–65)	4, 10, 24, 28, 34[b]	6.5	33.7	(24)
GD	Licorice confectionery	200	6	62.5 (57–72)	17	–48	–4.8	(22)
GA	1 capsule	500	6	69	3, 5, 11, 23	–17	13	(21)
GA	2 capsules	1000	6	69	3, 5, 11, 23	11	14	(21)
GA	3 capsules	1500	6	69	3, 5, 11,23	5.1	6.9	(21)

[a] Body weight of volunteers was not reported (NR). A mean body weight of 60 kg was assumed.
[b] Time of food intake was not reported. Times reflect an assumption of actual food consumption.

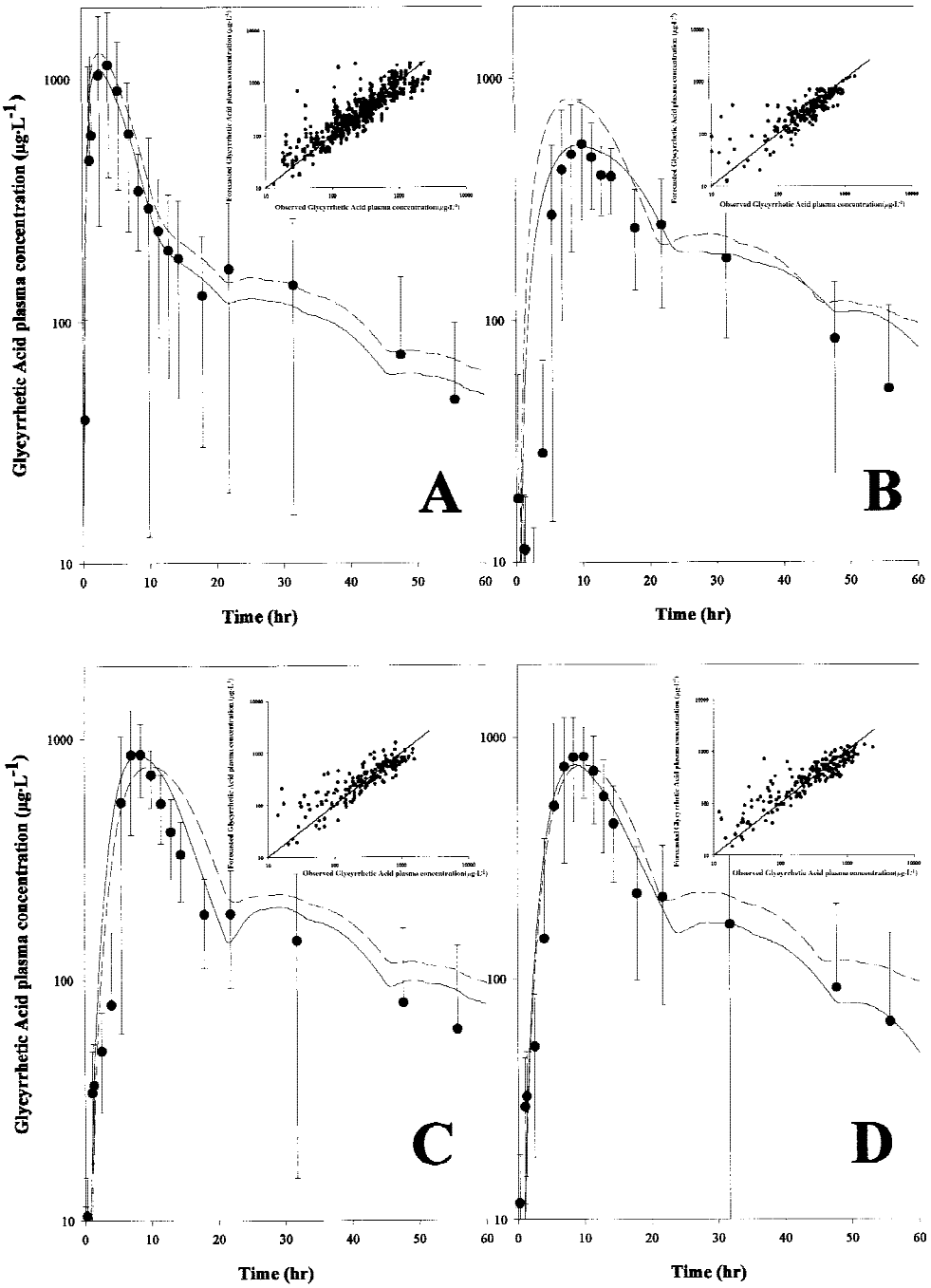

Fig. 2. The GA plasma concentration as a function of time after ingestion by 16 healthy human volunteers of (A) 130 mg GA as suspension; (B) 225 mg GD in solution; (C) 150 g sweet licorice containing 225 mg GD, and (D) 150 mg salted licorice containing 225 mg GD and 5% w/w NH_4Cl. The observed GA plasma concentration data (mean ± SD) are shown as symbols (●); the dashed and solid lines represent the forecast of the *a priori*-defined and the optimized model, respectively. The inserts in each panel show observed versus predicted GA plasma concentrations after optimization of the model.

ent from the fraction of a GD dose that is absorbed after the administration of either 225 mg GD as a solution (51% ± 22.7%) or as sweet (61% ± 17.4) or salted (58% ± 18.6%) licorice confectionery.

Of the four optimized parameters, only the T½ti showed a weak but significant correlation (Pearson correlation = 0.52) with the individually observed AUC of GA after the three GD treatments.

DISCUSSION

In the present study, a PBPK model is developed that successfully describes the GA plasma disposition after oral treatment with either GA or GD in humans. This model is based on a previously developed model for the rat (7), using specific knowledge on the human anatomy, physiology, and biochemistry. The GA kinetics in the human gastrointestinal

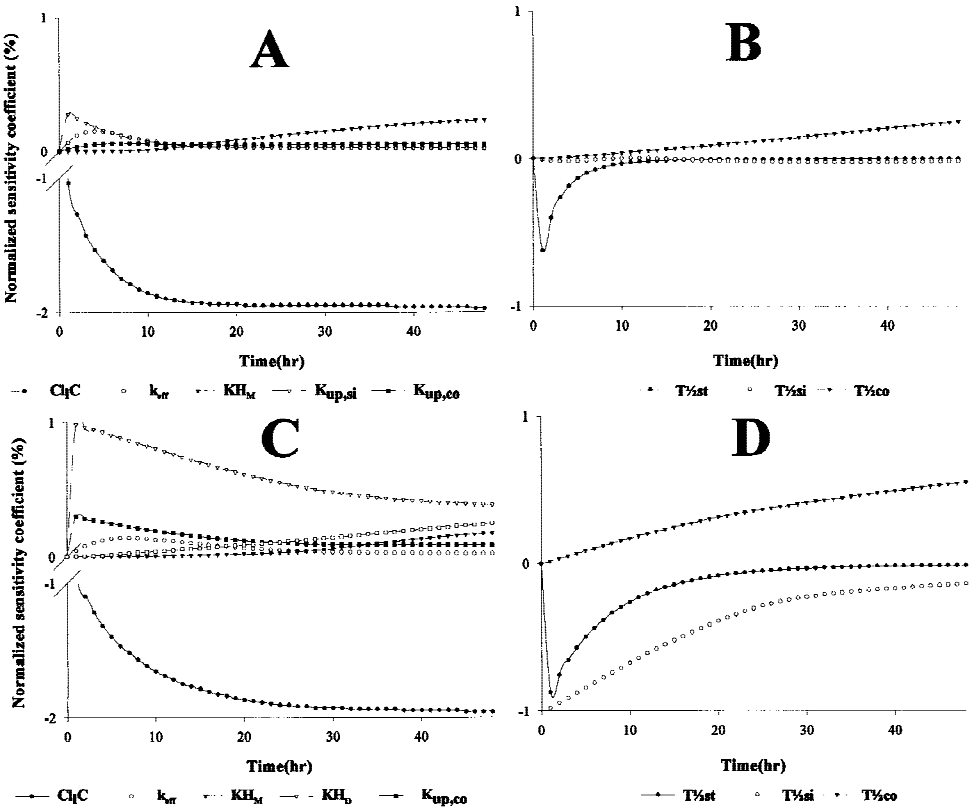

Fig. 3. The percentage change in the AUC as a function of time due to a charge of 1% in some model parameters of the PBPK model for GA in humans after single treatment of 130 mg GA in suspension (panels A and B), and 225 mg GD as licorice (panels C and D). For an explanation of abbreviations of the model parameters, see Table I.

tract were modeled by adding a gall bladder to the model. In addition, previously quantified differences in the canalicular transport of glucuronides in rats and humans (15) were used to quantify the biliary excretion of GA-glucuronides in humans. The *a priori* defined model adequately forecasts the plasma disposition of GA in human volunteers after oral treatment of either a suspension of GA, a GD solution, or the two licorice confectionery treatments. Although the model slightly overestimates the GA plasma concentrations after T_{max} the observed and predicted GA plasma concentrations closely resembled each other (inserts of Fig. 2). Furthermore, the model is able to forecast a second absorption peak, which was observed for the majority of the subjects (9,16) in the terminal phase of the plasma concentration time curve (Fig 2). This peak is attributed to the enterohepatic cycling of the biliary excreted GA metabolites. Taking into account that humans possess a gall bladder, information on the enterohepatic cycling in rats can be used to extrapolate this process in humans. As in rats, the enterohepatic cycling of GA glucuronides is of major influence on the human kinetics of GA. The good correspondence between the forecast and the observation justifies the assumption that the GA metabolites, following storage in the gall bladder, are excreted simultaneously into the gastrointestinal tract after the consumption of a meal containing fat (12). It is expected that the predicted and observed multiple absorption peak(s) will resemble one another even more closely when the meal consumption is exactly recorded during the entire study.

With the used optimization technique, it is not possible to consider the uncertainty in all model parameters simultaneously. Hence, the uncertainty in the four optimized parameters might be overestimated. However, this overestimation is expected to be minimal, since by optimization of only those parameters that have the most influence on the forecast, most of the uncertainty can be is explained (17). The observed difference in C_{max} and T_{max} after the GD solution and the two licorice confectionery treatments can be explained by a difference in the hydrolysis of GD in the gastrointestinal (GI) tract. This difference can be attributed to the presence of glucose in the licorice matrix, which might induce the bacterial activity in the GI tract.

Physiologically-based modeling of the gastrointestinal tract kinetics, as presented in this study, yields information on the fraction of the dose that is actually absorbed. Since this fraction is the same for all treatments, the systemic exposure to GA after either treatment with GA itself or GD in distinct matrices may be considered equal.

The presented human PBPK model for GD is adequately validated, since the model was able to forecast the GA plasma disposition properly under conditions that clearly differ from those of the calibration study. The relative residual between the observed and forecasted AUC and C_{max} after the oral administration of various GD doses remained below 17% for 5 out of 6 the previously published studies (Table IV). Nevertheless, the AUC and C_{max} are incomplete and indirect characteristics of the model output. Therefore, comparison of predicted and observed GA plasma concentration data is preferred. After modeling of the dissolution of GA in the small

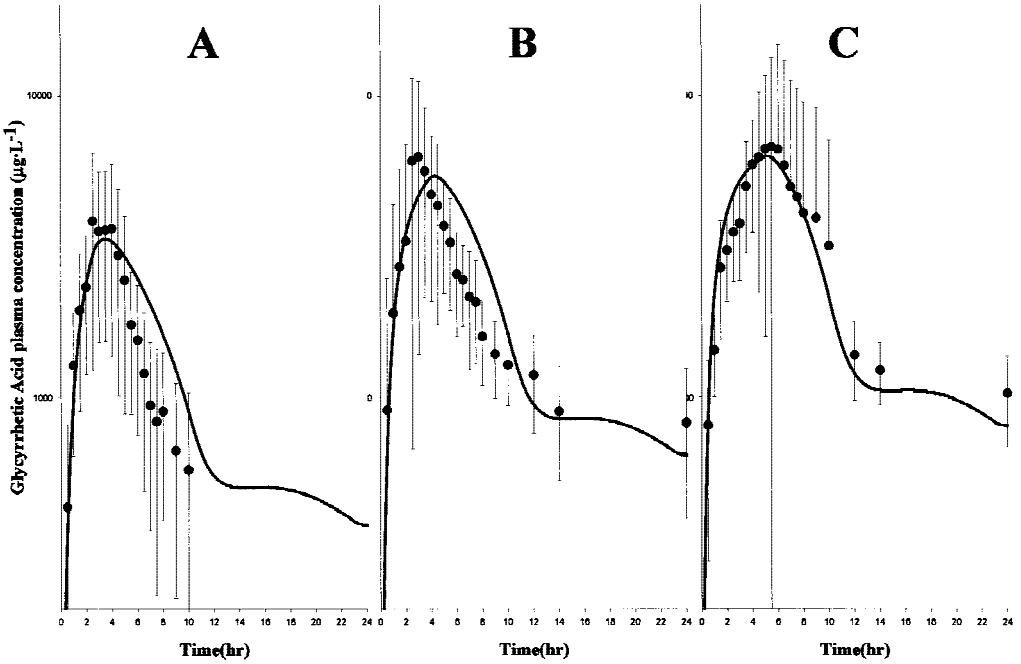

Fig. 4. The GA plasma concentration as a function of time after ingestion by six healthy human volunteers of (A) 500 mg GA; (B) 1000 mg GA, and (C) 1500 mg GA (data from (21)). The observed GA plasma concentration data (mean ± SD) are shown as symbols (●), whereas the solid lines represent the forecast of the optimized model.

intestine, the model appropriately forecasts the GA plasma concentrations after 1 to 3 capsules containing 500 mg GA per capsule (Table IV). The optimized solubility of GA (Cs) is lower than the theoretical aqueous solubility of the structural related compound carbenoxolone (25). This seems evident, since carbenoxolone—being the succinate ester of GA—was originally synthesized to improve the aqueous solubility of GA. However, the aqueous solubility of a compound does not necessarily reflect its solubility in the small intestine, since the physiological conditions in the gastrointestinal lumen may improve its solubility (20). The adapted model forecasts that after oral administration of doses of GA above 500 mg, only a fraction of the administered dose will dissolve and will consequently be available for absorption. This fraction decreases dose-dependent manner (70, 62, and 55% for a 500, 1000, and 1500 mg dose, respectively) and causes the observed dose-dependency in C_{max} (21). After high doses of undissolved GA, the concentration of GA in the small intestine, being dependent of its dissolution, uptake, and gastrointestinal transit, will approach its solubility and subsequently lower its dissolution rate. The dissolution rate of undissolved GA will become the rate-limiting step in the absorption of GA, which will result in the observed dose-dependency in T_{max} (21).

The ability of the model to forecast the GA plasma disposition after various oral treatments of either GA or GD indicates that the model can be used to simulate the GA kinetics after various exposure scenarios (6). If it is assumed that the toxicity of GA is directly correlated to its plasma disposition, the model might even be used to identify subgroups of the population that are at higher risk for licorice-induced toxicity. The chronic effect of GA on the conversion of cortisol to cortisone in the kidney, giving rise to the GA-induced hypertension and electrolyte disturbances, is reversible and associated with a regular intake (2). For cumulative toxicity, the AUC is generally regarded as an appropriate dose-metric (4). The T½ti shows a significant correlation with the individually observed AUC of GA after the 3 GD treatments. Although this correlation is weak and needs to be experimentally verified it can be expected that people with a delayed bowel movement will be at higher risk for licorice-induced adverse effects. In humans, the individual bowel movement can be easily obtained noninvasively (26). Hence, the bowel movement might serve as a practical risk-estimator. However, the correlation between the gastrointestinal transit rate and the AUC does not elucidate under which circumstances subjects are more at risk for licorice-induced side effects. In addition, other factors contribute to the observed interindividual differences in susceptibility (2). To completely quantify the interindividual variation, it is desirable to describe the relationship between the pharmacokinetics and pharmacodynamics in more detail (4). For such a relationship, an effect needs to be considered that is directly associated with the presence of GA, and which can be practically measured in humans. In the causal chain of licorice-induced hypertension and electrolyte disturbances, the inhibition of the enzyme 11-β-HSD is directly associated with the (over)consumption of licorice, and long-term inhibition of this enzyme may finally lead to hypertension (2,3). Inhibition of 11-β-HSD can be quantified noninvasively by determining the cortisol–cortisone ratio in 24-hr urine (27). However, detailed information on the relationship between GD exposure and its effect on this ratio is currently lacking. Finally, the relationship between the pharmacokinetics of orally ingested GD—oredicted by the presently developed human PBPK model—and its effect on the urinary cortisol–cortisone ratio may be used for the eventual PK/PD risk assessment of GD exposure.

ACKNOWLEDGMENT

The authors thank Dr. S. Krähenbühl (Department of Clinical Pharmacology; University of Bern) for making the raw data of the study of Krähenbuhl (21) available to us in numerical form.

REFERENCES

1. T. G. van Rossum, A. G. Vulto, R. A. de Man, J. T. Brouwer, and S. W. Schalm. Review article: Glycyrrhizin as a potential treatment for chronic hepatitis C. *Aliment. Pharmacol. Ther.* **12**:199–205 (1998).
2. F. C. Stormer, R. Reistad, and J. Alexander. Glycyrrhizic acid in liquorice—evaluation of health hazard. *Food Addit. Contam.* **31**: 303–312 (1993).
3. J. W. Funder, P. T. Pearce, R. Smith, and A. I. Smith. Mineralocorticoid action: target tissue specificity is enzyme, not receptor, mediated. *Science* **242**:583–585 (1988).
4. H. J. Clewell, 3rd and B. M. Jarnot. Incorporation of pharmacokinetics in noncancer risk assessment: Example with chloropentafluorobenzene. *Risk Anal.* **14**:265–276 (1994).
5. M. E. Andersen. Development of physiologically based pharmacokinetic and physiologically based pharmacodynamic models for applications in toxicology and risk assessment. *Toxicol. Lett.* **79**: 35–44 (1995).
6. M. E. Andersen, H. J. Clewell, 3rd, and C. B. Frederick. Applying simulation modeling to problems in toxicology and risk assessment—a short perspective. *Toxicol. Appl. Pharmacol.* **133**: 181–187 (1995).
7. B. A. Ploeger, J. Meulenbelt, and J. DeJongh. Physiologically based pharmacokinetic modeling of glycyrrhizic acid, a compound subject to presystemic metabolism and enterohepatic cycling. *Toxicol. Appl. Pharmacol.* **162**:177–188 (2000).
8. A. J. Coupe, S. S. Davis, and I. R. Wilding. Variation in gastrointestinal transit of pharmaceutical dosage forms in healthy subjects. *Pharm. Res.* **8**:360–364 (1991).
9. F. N. Christensen, S. S. Davis, J. G. Hardy, M. J. Taylor, D. R. Whalley, and C. G. Wilson. The use of gamma scintigraphy to follow the gastrointestinal transit of pharmaceutical formulations. *J. Pharm. Pharmacol.* **37**:91–95 (1985).
10. J. E. Devereux, J. M. Newton, and M. B. Short. The influence of density on the gastrointestinal transit of pellets. *J. Pharm. Pharmacol.* **42**:500–501 (1990).
11. D. A. Adkin, S. S. Davis, R. A. Sparrow, P. D. Huckle, A. J. Phillips, and I. R. Wilding. The effects of pharmaceutical excipients on small intestinal transit. *Br. J. Clin. Pharmacol.* **39**:381–387 (1995).
12. M. Lawson, G. T. Everson, W. Klingensmith, and F. Kern, Jr. Coordination of gastric and gallbladder emptying after ingestion of a regular meal. *Gastroenterology* **85**:866–870 (1983).
13. M. Proano, M. Camilleri, S. F. Phillips, M. L. Brown, and G. M. Thomforde. Transit of solids through the human colon: regional quantification in the unprepared bowel. *Am. J. Physiol.* **258**:G856–G862 (1990).
14. T. Akao. Hydrolysis of glycyrrhetyl mono-glucuronide to glycyrrhetic acid by glycyrrhetyl mono-glucuronide beta-D-glucuronidase of Eubacterium sp. GLH. *Biol. Pharm. Bull.* **20**: 1245–1249 (1997).
15. K. Niinuma, Y. Kato, H. Suzuki, C. A. Tyson, V. Weizer, J. E. Dabbs, R. Froehlich, C. E. Green, and Y. Sugiyama. Primary active transport of organic anions on bile canalicular membrane in humans. *Am. J. Physiol.* **276**:G1153–G1164 (1999).
16. S. Ishida, T. Ichikawa, and Y. Sakiya. Binding of glycyrrhetinic acid to rat plasma, rat serum albumin, humanserum, and human serum albumin. *Chem. Pharm. Bull.* **36**:440–443 (1988).
17. R. L. Dedrick. Animal scale-up. *J. Pharmacokinet. Biopharm.* **1**: 435–461 (1973).
18. M. V. Evans, W. D. Crank, H. M. Yang, and J. E. Simmons. Applications of sensitivity analysis to a physiologically based pharmacokinetic model for carbon tetrachloride in rats. *Toxicol. Appl. Pharmacol.* **128**:36–44 (1994).
19. P. Armitage and G. Berry, *Statistical methods in medical research,* Blackwell Science Ltd., Oxford, United Kingdom, 1994.
20. D. Horter and J. B. Dressman. Influence of physicochemical properties on dissolution of drugs in the gastrointestinal tract. *Adv. Drug Deliv. Rev.* **25**:3–14 (1997).
21. S. Krahenbuhl, F. Hasler, B. M. Frey, F. J. Frey, R. Brenneisen, and R. Krapf. Kinetics and dynamics of orally administered 18 beta-glycyrrhetinic acid in humans. *J. Clin. Endocrinol. Metab.* **78**:581–585 (1994).
22. S. Gunnarsdottir and T. Johannesson. Glycyrrhetic acid in human blood after ingestion of glycyrrhizic acid in licorice. *Pharmacol. Toxicol.* **81**:300–302 (1997).
23. K. Abe, A. Suzuki, H. Katayama, Y. Tatsumi, and E. Yumioka. Determination of 18 beta-glycyrrhetic acid in human plasma by high-performance liquid chromatography. *J. Chromatogr. B. Biomed. Appl.* **653**:112–115 (1994).
24. S. Takeda, H. Ono, Y. Wakui, A. Asami, Y. Matsuzaki, H. Sasaki, M. Aburada, and E. Hosoya. Determination of glycyrrhetic acid in human serum by high-performance liquid chromatography with ultraviolet detection. *J. Chromatogr. B. Biomed. Appl.* **530**:447–451 (1990).
25. J. Blanchard, L. M. Tang, and M. E. Earle. Reevaluation of the absorption of carbenoxolone using an in situ rat intestinal technique. *J. Pharm. Sci.* **79**:411–414 (1990).
26. K. W. Heaton and L. O'Donnell. An office guide to whole-gut transit time. Patients' recollection of their stool form. *J. Clin. Gastroenterol.* **19**:28–30 (1994).
27. R. Best and B. R. Walker. Additional value of measurement of urinary cortisone and unconjugated cortisol metabolites in assessing the activity of 11 beta-hydroxysteroid dehydrogenase in vivo. *Clin. Endocrinol.* **47**:231–236 (1998).
28. R. Brown, J. Foran, S. Olin, and D. Robinson. *Physiological parameter values for PBPK models,* International Life Sciences Institute and Risk Science Institute, Washington DC, 1994.
29. International Commission of Radiological Protection (ICRP), *Publication 23: Report of the Task Group on Reference Man,* Pergamon Press, New York, 1975.

APPENDIX

Mass Balance Differential Equations (For abbreviations, see Table I)

Change of amount in:

Venous Plasma: $$\frac{d}{dt}A_v = Q_l + Q_g \cdot C_{vl} + Q_r \cdot C_r/P_r - Q_c \cdot C_v \quad (1)$$

Arterial Plasma: $$\frac{d}{dt}A_a = Q_c \cdot C_v - C_a \quad (2)$$

Remaining Tissue: $$\frac{d}{dt}A_r = Q_r \cdot (C_a - C_r/P_r) \quad (3)$$

Venous Liver Plasma: $$\frac{d}{dt}A_{vl} = Q_l \cdot C_a + Q_g \cdot (C_g/P_g) - (Q_l + Q_g) \cdot C_{vl} - \frac{d}{dt}A_{up} - \frac{d}{dt}A_{out} + K_{eff} \cdot A_l \quad (4)$$

Liver Tissue: $$\frac{d}{dt}A_l = \frac{d}{dt}A_{up} - K_{eff} \cdot A_l \quad (5)$$

Gut Tissue: $$\frac{d}{dt}A_g = Q_g \cdot (C_a - C_g/P_g) + \frac{d}{dt}Aup_A + \frac{d}{dt}Aup_{DM} \quad (6)$$

Stomach Lumen:

GA: $$\frac{d}{dt}A_{A,st} = \frac{Dose_A}{2 \cdot T½st} \quad (7)$$

GD: $$\frac{d}{dt}A_{D,st} = \frac{Dose_D}{2 \cdot T½st} \quad (8)$$

Small & Large Intestinal Lumen:

GA: $$\frac{d}{dt}A_{A,ti} = -\frac{d}{dt}A_{A,st} - \frac{d}{dt}Aup_A - \frac{d}{dt}A_{A,fe} \quad (9)$$

GD: $$\frac{d}{dt}A_{D,ti} = -\frac{d}{dt}A_{D,st} - \frac{d}{dt}H_D - \frac{d}{dt}A_{D,fe} \quad (10)$$

GA metabolites (GM): $$\frac{d}{dt}A_{M,ti} = -\frac{d}{dt}H_M - \frac{d}{dt}A_{M,fe} \quad (11)$$

Hydrolyzed GD and GM:

$$\frac{d}{dt}A_{DM,ti} = \frac{d}{dt}H_D + \frac{d}{dt}H_M - \frac{d}{dt}Aup_{DM} - \frac{d}{dt}A_{DM,fe} \quad (12)$$

Feces:

GA: $$\frac{d}{dt}A_{A,fe} = \frac{Dose_A}{2 \cdot T½ti} \quad (13)$$

GA: $$\frac{d}{dt}A_{D,fe} = \frac{Dose_D}{2 \cdot T½ti} \quad (14)$$

Hydrolyzed GD and GM: $$\frac{d}{dt}A_{DM,fe} = \frac{A_{DM,co}}{2 \cdot T½co} \quad (15)$$

Change of Amount Transported Into:

Liver Tissue: $$\frac{d}{dt}A_{up} = Cl_l \cdot C_{vl} \cdot f_u \quad (16)$$

Bile: $$\frac{d}{dt}A_{out} = Cl_l \cdot C_{vl} \cdot f_u \quad (17)$$

Amount Stored in Gall Bladder Between Two Successive Meal Ingestions at Time $t = t_z$ *and* $t = t_{z+1}$:

$$A_{gb} = \int_{t=t_z}^{t=t_{z+1}} \frac{d}{dt}A_{out} \quad (18)$$

Emptying of Gall Bladder at Ingestion of a Meal Containing Fat:

$$A_{M,ti} = A_{M,ti} + A_{gb} \quad (19)$$

$$\frac{d}{dt}A_{M,fe} = \frac{A_{M,ti}}{2 \cdot T½ti} \quad (20)$$

$$A_{gb} = 0;\ z = z + l$$

Amount Absorbed From GI tract:

GA: $$\frac{d}{dt}Aup_A = K_{up} \cdot A_{A,ti} \quad (21)$$

Hydrolyzed GD and GA Metabolites (GM):

$$\frac{d}{dt}Aup_{DM} = K_{up} \cdot A_{DM,ti} \quad (22)$$

Amount Hydrolyzed In the GI Tract:

GD: $$\frac{d}{dt}H_D = KH_D \cdot A_{D,ti} \quad (23)$$

GM: $$\frac{d}{dt}H_M = KH_M \cdot A_{M,ti} \quad (24)$$

The Dissolution of Ga in the GI Tract; Amount:

GA Dissolved (Noyes–Whitney Equation):

$$\frac{d}{dt}Adis_{ti} = Ks \cdot n_{cap} \cdot (Cs - A_{A,ti}/V_{co}) \quad (25)$$

Undissolved GA in Small and Large Intestines:

$$\frac{d}{dt}As_{ti} = \frac{d}{dt}A_{A,st} - \frac{d}{dt}As_{A,fe} - \frac{d}{dt}Adis_{ti} \quad (26)$$

Dissolved GA in Small and Large Intestines:

$$\frac{d}{dt}A_{A,ti} = \frac{d}{dt}Adis_{ti} - \frac{d}{dt}Aup_A - \frac{d}{dt}A_{A,fe} \quad (27)$$

Undissolved GA in the Feces: $$\frac{d}{dt}As_{fe} = \frac{As_{ti}}{2 \cdot T½si} \quad (28)$$